

## A nonlinear model for AC induced corrosion

N. Ida<sup>1\*</sup>, Y. Le Menach<sup>2</sup>, X. Shan<sup>3</sup> and J. Payer<sup>4</sup>

<sup>1</sup>The University of Akron, Department of Electrical and Computer Engineering, Akron, OH, 44325, USA

<sup>2</sup>L2EP, Universite Lille 1, 59655 Villeneuve d'Ascq, France

<sup>3</sup>Research and Engineering Center, Whirlpool, Benton Harbour, MI, 49022, USA

<sup>4</sup>The University of Akron, Corrosion and Reliability, Akron, OH, 44325, USA

\*corresponding author, E-mail: [ida@uakron.edu](mailto:ida@uakron.edu)

### Abstract

The modeling of corrosion poses particular difficulties. The understanding of corrosion as an electrochemical process has led to simple capacitive-resistive models that take into account the resistance of the electrolytic cell and the capacitive effect of the surface potential at the interface between conductors and the electrolyte. In some models, nonlinear conduction effects have been added to account for more complex observed behavior. While these models are sufficient to describe the behavior in systems with cathodic protection, the behavior in the presence of induced AC currents from power lines and from RF sources cannot be accounted for and are insufficient to describe the effects observed in the field. Field observations have shown that a rectifying effect exists that affects the efficacy of cathodic protection and this effect is responsible for corrosion in the presence of AC currents. The rectifying effects of the metal-corrosion interface are totally missing from current models. This work proposes a nonlinear model based on finite element analysis that takes into account the nonlinear behavior of the metal-oxide interface and promises to improve modeling by including the rectification effects at the interface.

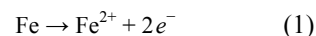
### 1. Introduction

Induced alternating current (AC) degradation has become more widely recognized as a threat to the integrity of underground structures, e.g. pipelines co-located with high-voltage transmission lines, AC-powered rail transit systems, and structures where there are stray AC currents. However, the mechanisms of AC corrosion are still not well understood. Of interest are discernment of the processes of Alternating Current (AC) induced corrosion and interactions with cathodic protection systems. A primary focal point is the effect of surface films and corrosion products of metals on the modulation of the AC/DC currents. Metal-oxide-metal (MOM) junctions can have semiconductor properties and nonlinear effects on the currents.

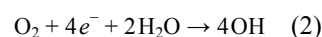
Corrosion is an electrochemical process, and the electrolytic cell can be described as a dc phenomenon. At the anode, metal is consumed and soluble ions and electrons

are produced by an oxidation reaction. At the cathode, a reducible species, e.g. hydrogen ions or oxygen, is consumed along with electrons. Electrons leave the anode and transfer by electronic conductivity to the cathode. The electrolytic cell is completed by transport of ions through the electrolyte by ionic conductivity. The transfer of electrons generated by the anodic reaction balances the electrons consumed by the cathodic reaction.

The process involved in corrosion of iron and formation of corrosion products is as follows [1]. The oxidation of iron results in formation of ferrous ions and generation of electrons:

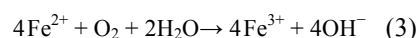


Oxygen either in air or in solutions, including moist soil provides the reducible species for a reduction on the metal surface. Oxygen is consumed, electrons are consumed and hydroxyl ions are produced.

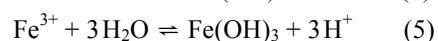
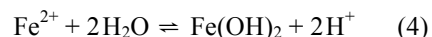


The generation of hydroxide ions ( $\text{OH}^{-}$ ) makes the reaction sensitive to the pH of the environment.

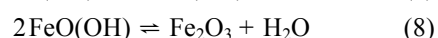
A redox reaction occurs in the presence of water and results in formation of corrosion products:



The following acid-base reactions occur as well:



Followed by the dehydration equilibria:



These reactions describe the formation of different corrosion products, and FeO and  $\text{Fe}_2\text{O}_3$  are only two out of

some 16 different corrosion products of iron. The corrosion environment determines the reactions under different conditions and leads to these products. For example, under water, in oxygen-poor environments, the primary corrosion product is  $Fe_3O_4$  (magnetite). The latter, in the presence of oxygen converts into  $Fe_2O_3$ .

Cathodic protection (CP) is a common method to mitigate corrosion of steel structures in soil and waters. As shown in the reaction in (1), if the flow of electrons from the iron can be stopped corrosion cannot occur. A source of potential that is sufficiently negative will stop the flow of electrons. The principle of cathodic protection is shown in Fig. 1 does exactly that. In Fig. 1a, a DC source is connected so that flow of electrons from the source counters the flow of electrons from iron. This method is called impressed current cathodic protection. Another method of cathodic protection shown in Fig. 1b, is termed passive or sacrificial cathodic protection. A sacrificial metal with more negative contact potential, typically zinc is used and connected to the iron being protected. This forms a cell and as long as the zinc is not entirely consumed, the iron item is protected from corrosion.

Because the process of corrosion and the cathodic protection are DC processes it has been assumed that only DC currents can produce corrosion. However, it has been known for some time that AC induced currents not only affect the rate of corrosion but also alter the DC currents and potentials and hence can accelerate the rate of corrosion [2,3]. There is anecdotal evidence that high frequency fields produced by antennas can also affect corrosion rates [4,5]. The fundamental model for corrosion currently in use is the capacitive-resistive model in Fig. 2. The model takes into account the nonlinear impedance of the double layer at the interface through use of the capacitance and resistance (a nonlinear polarization impedance) and a fixed soil resistance  $R_s$ . More complex models that include rectifying elements have been proposed [6]. The existence of rectification mechanisms in corrosion has been identified earlier as an electromagnetic interference effect near transmitting antennas in what is known as the “rusty bolt effect” [7], whose model is shown in Fig. 3. The nonlinear clipping effect of this circuit is at the base of the observed interference signals re-radiated by the corroded structures and confirms the fact the corrosion products are semiconducting. The net effect is a metal-oxide-metal (MOM) diode, a construct that indicates that these structure can affect the CP conditions through rectification. The rectification process gains some strength considering the fact that iron oxides are all semiconducting hence the creation of metal-oxide junctions is a fact. In the case of buried pipes, the oxide layer is between iron on the one side and soil on the other, both conducting but asymmetric (i.e., the iron-iron oxide junction is different than the soil-iron oxide junction). This construct is very similar to metal-oxide-metal junctions, devices that are being studied specifically for their rectification properties, especially at higher frequencies.

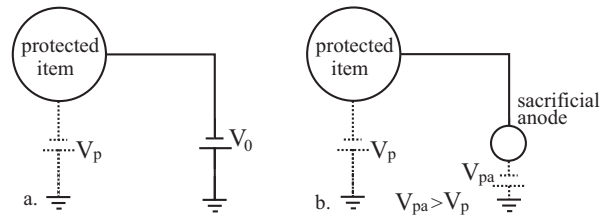


Figure 1: Cathodic protection. a. Active protection.  $V_0 > V_p$  where  $V_p$  is the contact potential of the protected item (iron). b. Passive cathodic protection. The sacrificial metal provides the potential  $V_{pa}$  to counter the flow of electrons from the protected item provided  $V_{pa} > V_p$ .

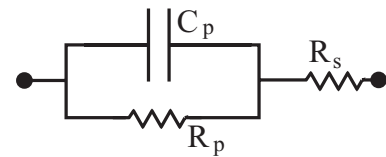


Figure 2: The basic current model for corrosion.

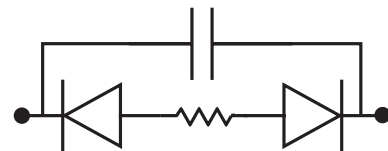
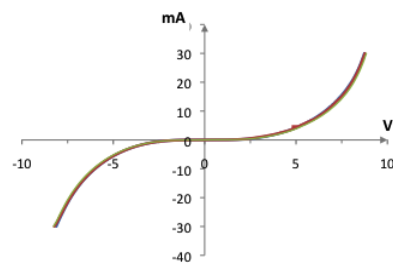
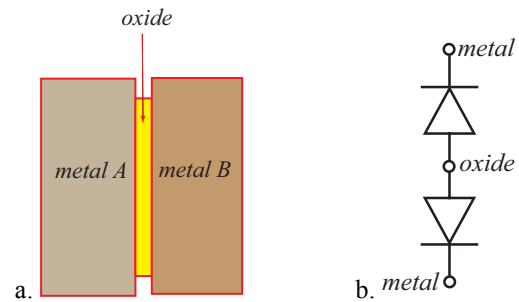


Figure 3: The rusty bolt effect – model.



c.

Figure 4: The metal-oxide-metal experiment. a. Two steel disk with iron oxide grown on their facing surfaces. b. The MOM diode model. c. The  $I-V$  characteristics obtained.

$$\mathbf{E} = \rho(|\mathbf{J}|)\mathbf{J} \quad (12)$$

Experimental work. To verify that corrosion on the surface of metals in soil does form a back-to-back diode configuration it is sufficient to grow iron oxide (Fe<sub>2</sub>O<sub>3</sub>) on two metal surfaces, place them face to face and subject them to an I–V test. This experiment is shown in Fig. 4 where two small disks are used. The I–V characteristics of this configuration is shown in Fig. 4c clearly indicating the back-to-back diode effect and the fact that the backward avalanche region is around 7.5V in both direction. Other corrosion products, such as magnetite (Fe<sub>3</sub>O<sub>4</sub>) can be similarly evaluated. In an actual corrosion environment, one metal would typically be steel whereas the other is the soil itself and the behavior in Fig. 4c is expected to be asymmetric.

## 2. The numerical model

To derive an appropriate numerical model we assume that eddy currents are induced in the conducting structures and that the presence of the semiconducting layer requires nonlinear treatment of its conductivity. We consider the eddy-current problem shown in Fig. 5 where the current in the domain  $\mathcal{D}$  enters through the surface  $\Gamma_{t1}$  and exits through the surface  $\Gamma_{t2}$ . In our case the domain  $\mathcal{D}$  is conducting everywhere ( $\rho \neq 0$ ).

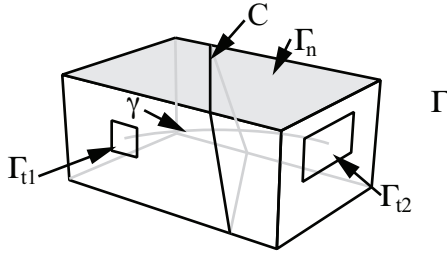


Figure 5: The general eddy-current problem

To model an eddy-current problem, it is necessary to solve Maxwell's equations neglecting displacement currents. With this condition, Maxwell's equations are reduced to:

$$\nabla \times \mathbf{H} = \mathbf{J} \quad (9)$$

$$\nabla \times \mathbf{E} = \partial_t \mathbf{B} \quad (10)$$

where  $\mathbf{H}$  is the magnetic field intensity,  $\mathbf{E}$  the electrical field intensity,  $\mathbf{J}$  the current density and  $\mathbf{B}$  the magnetic flux density. The conservation of the flux must be ensured such that  $\nabla \cdot \mathbf{J} = 0$  and  $\nabla \cdot \mathbf{B} = 0$ .

The boundary conditions are defined such that  $\mathbf{B} \cdot \mathbf{n} = 0$  on  $\Gamma$ ,  $\mathbf{J} \cdot \mathbf{n} = 0$  on  $\Gamma_n$  and  $\mathbf{E} \times \mathbf{n} = 0$  on  $\Gamma_t$ .

Associated with Maxwell's equations are the constitutive relations:

$$\mathbf{B} = \mu \mathbf{H} \quad (11)$$

In the case treated here the magnetic material properties are linear but the semi-conductor conductivity is non linear.

Equations (9) through (12) can be combined in well-known formulations in terms of  $\mathbf{E}$  or  $\mathbf{H}$ . Here, we propose a formulation in terms of potentials, called the  $\mathbf{T}$ - $\Omega$  formulation where  $\mathbf{T}$  is the electric vector potential and  $\Omega$  is the magnetic scalar potential.

The current density  $\mathbf{J}$  can be decomposed into two terms  $\mathbf{J}_0$ , representing the externally imposed current density and  $\mathbf{J}_{eddy}$ , representing the induced currents. The electric vector potential can be define such that:

$$\nabla \times \mathbf{T} = \mathbf{J}_{eddy} \quad (13)$$

In the physical environment,  $\mathbf{J}_0$  is the source of induced currents such as power lines whereas  $\mathbf{J}_{eddy}$  represent the induced currents in the metal structure in which corrosion is modeled. To satisfy the boundary conditions on  $\mathbf{J}$  and  $\mathbf{E}$  the condition  $\mathbf{T} \times \mathbf{n} = 0$  on  $\Gamma_n$  must be enforced.  $\mathbf{J}_0$  can be set from a vector field  $\mathbf{N}$  that must satisfy the following conditions:

$$\left\{ \begin{array}{l} \int_{\Gamma_{ii}} \mathbf{N} \cdot d\mathbf{s} = \pm 1 \\ \int_{\Gamma_m} \mathbf{N} \cdot d\mathbf{s} = 0 \\ \nabla \cdot \mathbf{N} = 0 \end{array} \right\} \quad (14)$$

With these conditions we can write  $\mathbf{J}_0 = \mathbf{N}i$  where  $i$  is a sinusoidal current function. From  $\mathbf{N}$  we can introduce a vector  $\mathbf{K}$  such that:

$$\left\{ \begin{array}{l} \oint_C \mathbf{k} \cdot d\mathbf{l}_s = \pm 1 \\ \nabla \times \mathbf{K} = \mathbf{N} \end{array} \right\} \quad (15)$$

Equation (9) can now be re-written with these introduced terms:

$$\nabla \times \mathbf{H} = \mathbf{J}_0 + \mathbf{J}_{eddy} = \mathbf{N}i + \nabla \times \mathbf{T} \rightarrow \nabla \times (\mathbf{H} - \mathbf{T} - \mathbf{K}i) = 0 \quad (16)$$

Form this form it is possible to introduce the magnetic scalar potential as follows:

$$\mathbf{H} - \mathbf{T} - \mathbf{K}i = -\nabla \Omega \quad (17)$$

To ensure the uniqueness of  $\Omega$ , a value at a point of  $\mathcal{D}$  must be fixed.

Finally, after combining (10), (11), (12) and (17) we obtain a new form of Maxwell-Faraday relationship:

$$\rho(|\mathbf{J}|) \cdot \nabla \times \nabla \times \mathbf{T} + \mu \partial_t (\mathbf{T} + \mathbf{K}i - \nabla \Omega) = 0 \quad (18)$$

In addition it is necessary to ensure the zero divergence of **B**. The latter follows directly from (17):

$$\nabla \cdot \mu(\mathbf{T} + \mathbf{K}i - \nabla\Omega) = 0 \quad (19)$$

To use the finite element method, the formulation **T-Ω** must be converted into the equivalent weak formulation [8]. The vector potential **T** and the vector field **K** are discretized on the edges of the finite element mesh using the Whitney complex [8]. The scalar potential **Ω** is defined at the nodes of the mesh.

It should be noted that the formulation in the continuous domain does not guarantee a unique solution but uniqueness is guaranteed in the discrete, finite element domain. Since we need to find  $\nabla \times \mathbf{T}$  and  $\nabla \Omega$ , the actual values of **T** and **Ω** are of no interest.

### 3. Non-linear model

As indicated above, the model is non-linear due to the semiconducting layer. The measurements are carried out across the semiconductor layer. A voltage is imposed across the two conductors and the current through the semiconducting layer is measured. **Figure 6** shows the electrical field **E** in the sheet based on the current density through the sheet.

To model the semiconductor we use a simple regression. The relationship between *E* and *J* is  $E = aJ^b$  with *a* and *b* respectively equal 6081 and 0.301. These values were extracted from the experimental measurements since no data on the nonlinear behavior of metal oxide junctions could be found. Obviously, other junctions will have characteristics and these need to be established.

The solver used to obtain the non-linear solution is the fixed-point method.

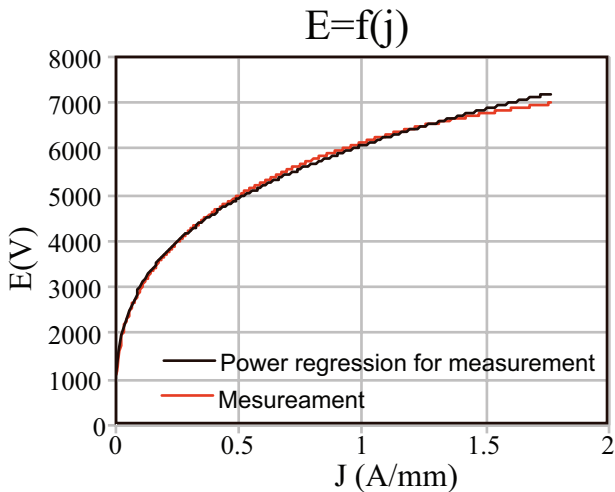


Figure 6: Electrical field as a function of current density in the semiconducting layer.

### 4. Results

The nonlinear model above was applied to a simple geometry that duplicates the experimental configuration in **Fig. 4a** with  $i = 5 \times 10^{-3} \sin(\omega t)$  the current imposed through the model and **K** a vector field such that  $\nabla \times \mathbf{K} = \hat{y}$ . The model is shown in **Fig. 7** and is made of two steel disks and a semiconducting layer (black) sandwiched between them. The figure shows as well the finite element mesh (only the elements on the outer surface are visible). The current distribution in the middle of the model is shown in **Fig. 8**. The skin depth in steel is clearly visible. **Fig. 9** is the terminal voltage showing the nonlinear effect of the semiconducting layer. This waveform has been previously observed in work on the rusty bolt effect [7]

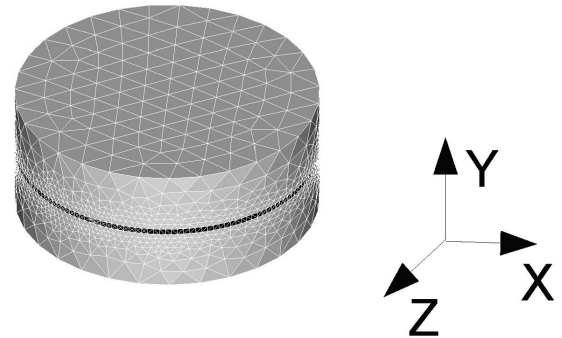


Figure 7: The model used for computation. The finite element mesh can be seen on the surface. The iron oxide layer is sandwiched between two steel disks.

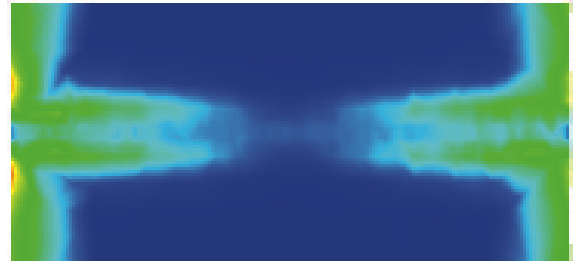


Figure 8: Current distribution in the model.

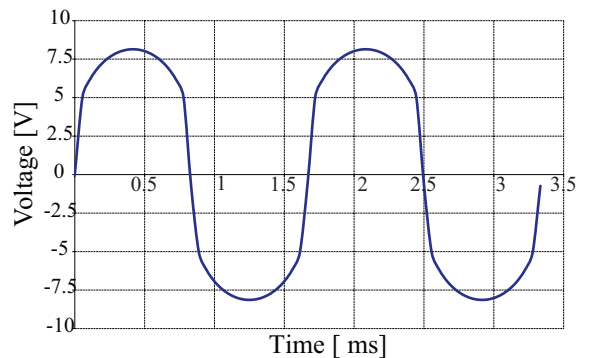


Figure 9: Evolution in time of the terminal voltage.

## 5. Conclusions

A simple nonlinear model based on the formulation of Maxwell's equations in terms of the electric vector potential  $T$  and magnetic scalar potential  $W$  with nonlinear conductivity has been presented for the purpose of modeling corrosion. The nonlinearity is derived from experimental data. The results show the expected characteristics of clipped sinusoidal voltage that has been observed in work on the rusty bolt effect. The current model is expected to provide a means of more accurate modeling of the effects observed in corrosion in pipes and other structure by the introduction of the rectification effects.

## References

1. H. Gräfen, E.M. Horn, H. Schlecker and H. Schindler, H. "Ullmann's Encyclopedia of Industrial Chemistry," Wiley, 2000.
2. S. Goidanich, L. Lazzari and M. Ormellese "AC corrosion. Part 2: Parameters influencing corrosion rate," *Corrosion Science*, Vol. 52, 916–922, 1986.
3. R. Zhang, P.R. Vairavanathan and S.B. Lalvani, "Perturbation method analysis of AC induced corrosion," *Corrosion Science*, Vol. 50, 1664-1671, 2008.
4. N. Ida, J. H. Payer, and X. Shan, "Electromagnetic Radiation Effects on Corrosion," in Proceedings of the DoD Corrosion Conference, July 31 – August 5, 2011.
5. J. H. Payer, N. Ida, and X. Shan "AC-Induced Corrosion and Interactions with Cathodic Protection," in Proceedings of the DoD Corrosion Conference, July 31 – August 5, 2011.
6. I. Ibrahim, M. Meyer, B. Tribollet, H. Takenouti, S. Joiret, S. Fontaine and H.G. Schoneich, "On the mechanism of AC assisted corrosion of buried pipelines and its CP mitigation," Proc. IPC, 1-25, 2008.
7. R. Haynes, H.W. Carhart and J.C. Cooper, "Chemical reduction of intermodulation interference caused by metal-oxide-metal junctions aboard ships," Naval Research Laboratory report AD-A239 530, July 31, 1991.
8. A.Bossavit, "Electromagnétisme en vue de la modélisation", édition Springer-Verlag, 1993.